The Parameterization of Sampling Errors in Infrared Sea Surface Temperatures

Yang Liu[(1)], Toshio Chin[(2)], Peter Minnett[(1)]

(1) Department of Ocean Sciences, Rosenstiel School of Marine and Atmospheric Science, University of Miami, Miami, Florida, USA

(2) Jet Propulsion Laboratory, NASA, Pasadena, California, USA

Introduction

Clouds and inter-swath gaps are the primary reasons for incomplete coverage of satellite infrared (IR) measurements of the Earth's surface, and yield sampling errors in averaged IR Sea-surface Temperature (SST) fields.

In a recent paper (Liu & Minnett. 2016; hereafter referred to as LM16) we found that the MODIS (Moderate Resolution Imaging Spectroradiometer (Esaias et al. 1998)) monthly SST sampling error referenced to MUR SSTs (Multi-scale Ultrahigh Resolution (Chin et al. 2010), is up to O(1 K), which far exceeds the error threshold needed for climate research.

The next question to ask is, can the sampling errors be predicted? In reality, when assessing sampling errors in satellite-derived IR SST fields we do not have an appropriate reference field at the various temporal and spatial averaging intervals. However, we do have access to a number of relevant variables that can be used with the results of LM16 to estimate the sampling errors, for example in terms of the local SST difference from a reference, gap fraction, cloud persistence (the number of consecutive days during which a location is detected to be cloudy), or season and region.

SST Sampling Errors

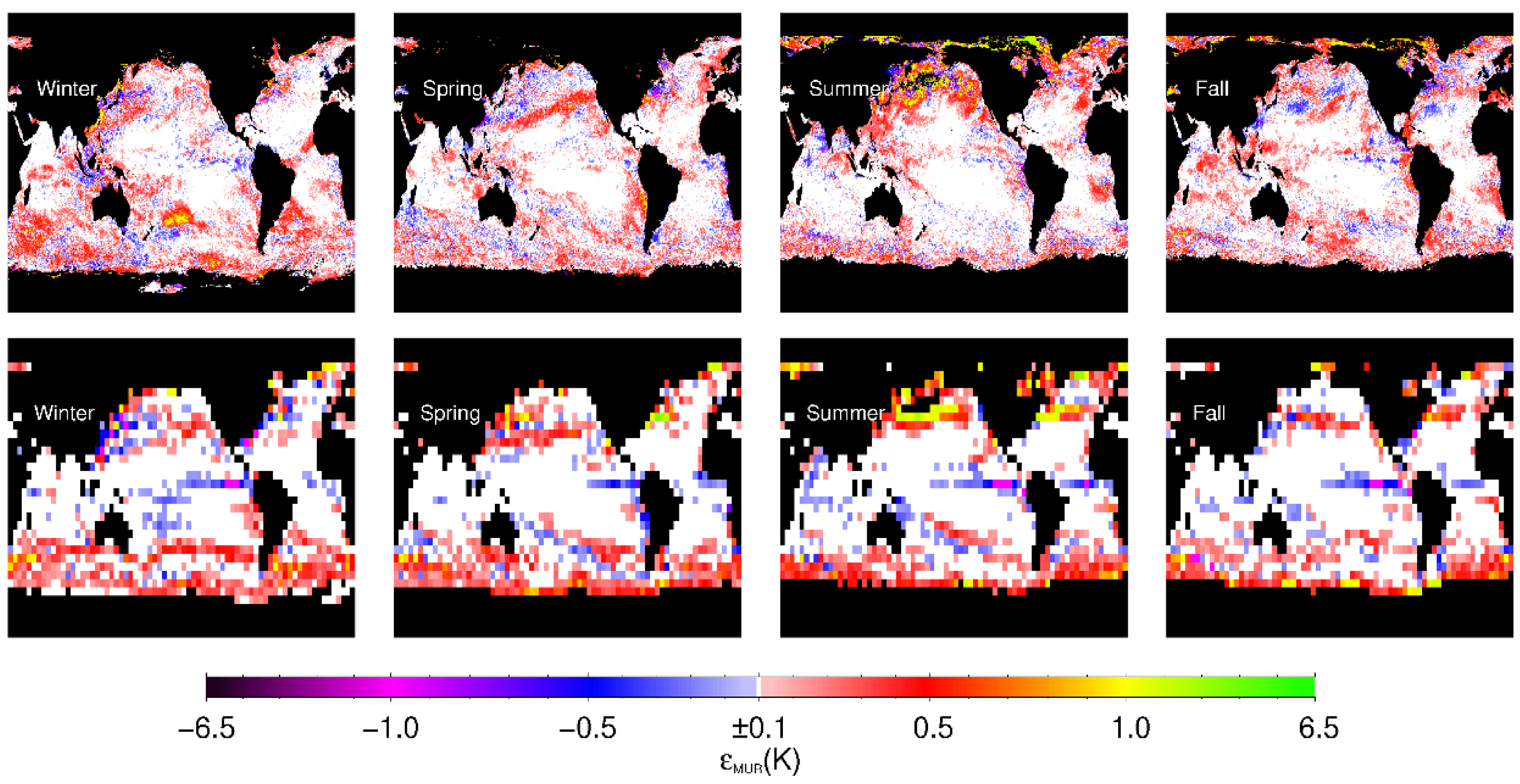

Figure 1. Sampling errors generated using MUR SST. Upper: temporal averaging of [0.25, mon]; lower: spatial averaging of [5, 1d]. Boreal seasons are denoted on the Asian continent.

The Climatology Component

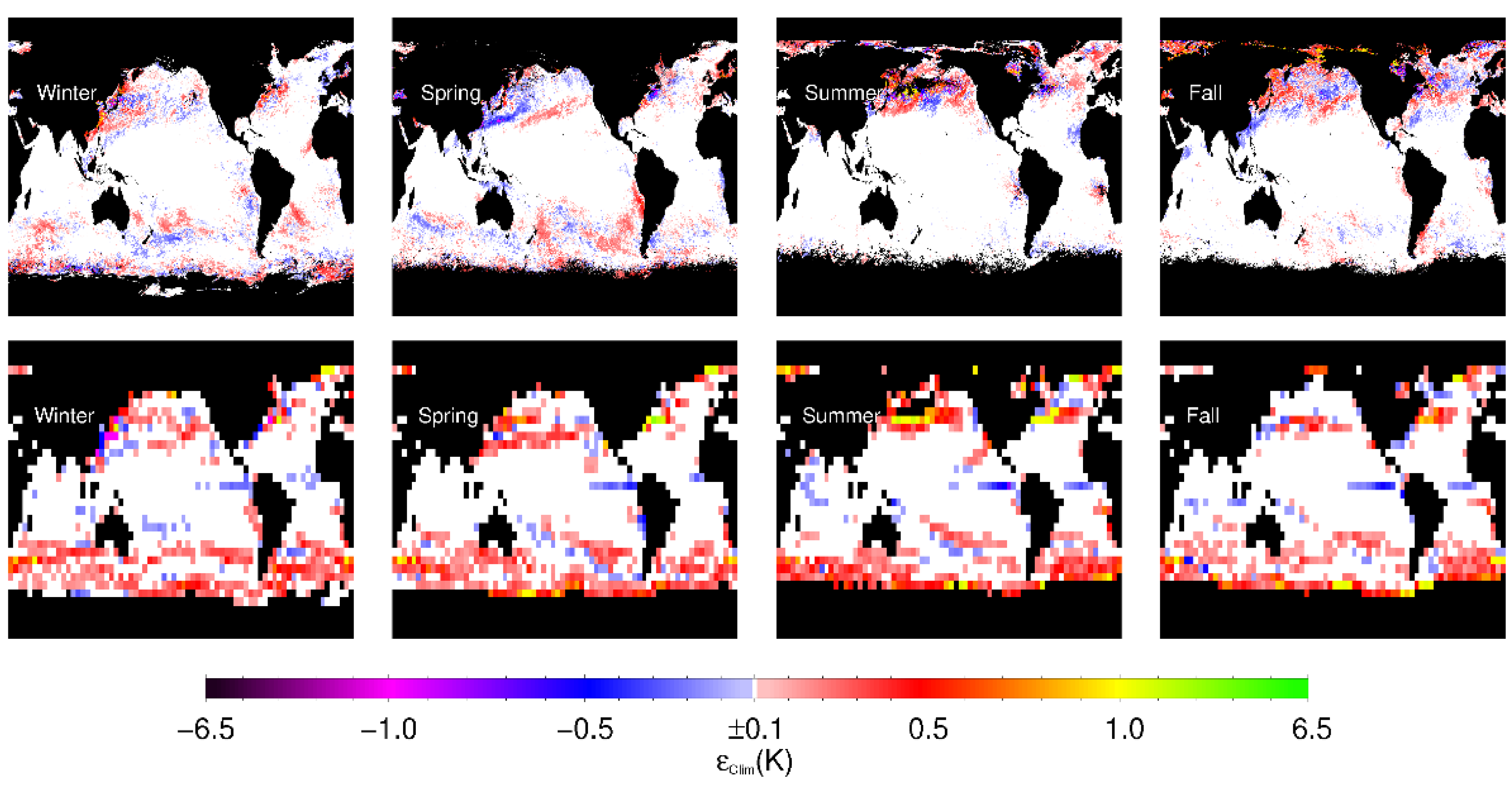

Figure 2. Sampling errors generated using OISST climatology. Upper: temporal averaging of [0.25º, mon]; lower: spatial averaging of [5, 1d]. Boreal seasons are denoted on the Asian continent.

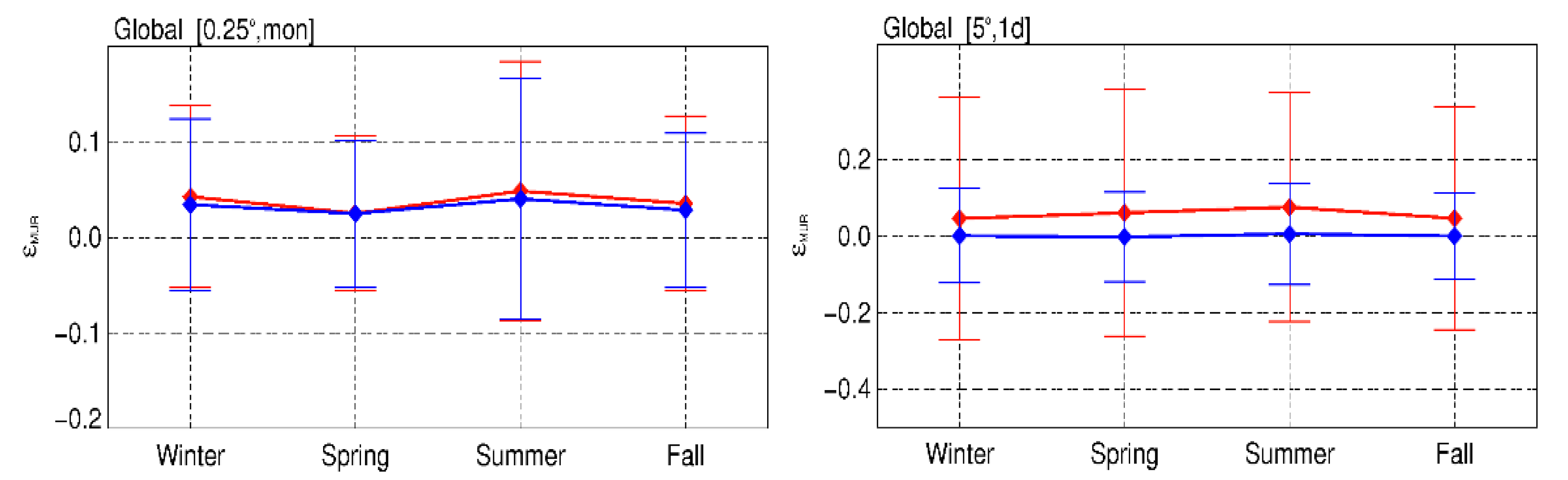

Figure 3. Global seasonal sampling errors quantified using MUR SSTs (red) and MUR SST anomalies (blue).

The sampling errors quantified using MUR SST anomalies calculated using the OISST climatology (Banzon et al, 2014) as the reference are smaller, especially in spatial averages that both mean error and RMSE are substantially (>90% mean ERR and >50% RMSE) reduced after the seasonal signals are removed. However, the RMSE and the mean error barely change magnitudes after the removal of the climatology.

Error Parameterization

As a preliminary exploration, we assume the error function can take the form:

$$\varepsilon_m = \alpha_0 \varepsilon_{clim} + (\alpha_1 f^{\alpha 2} + \alpha_3 \hat{p}^{\alpha 4})\sigma + \alpha_5$$

where α_0, α_1, α_2, α_3, α_4, α_5, are coefficients found by a Levenberg-Marquardt algorithm to reach a non-linear least squares fit; $\alpha_3 = 0$ in spatial sampling error estimates, f is the gap fraction ($0 < f < 1$), $\hat{p}$ is the normalized cloud persistence ($0 < \hat{p} < 1$), and σ is the standard deviation of the SSTs in the averaging grid cell from MUR (σ_{MUR}). We also test the model using SST standard deviation of the climatology (σ_{clim}). When σ_{clim} is applied, the model computes the sampling error estimates $\varepsilon_m{}'$ without any inputs from a Level 4 reference field and thus is predictive.

For the positive sampling errors, which primarily exist in mid- and high-latitudes and the stratocumulus regions, ε_m shows overall improvement.

Figure 4 and 5 exhibit that the improvements are primarily in positive sign sampling errors, which is because the model can not predict both positive and negative errors with the same set of gap fractions, cloud persistence and SST standard deviation.

Therefore, the fitting is better when only error absolute values are estimated (Figure 6).

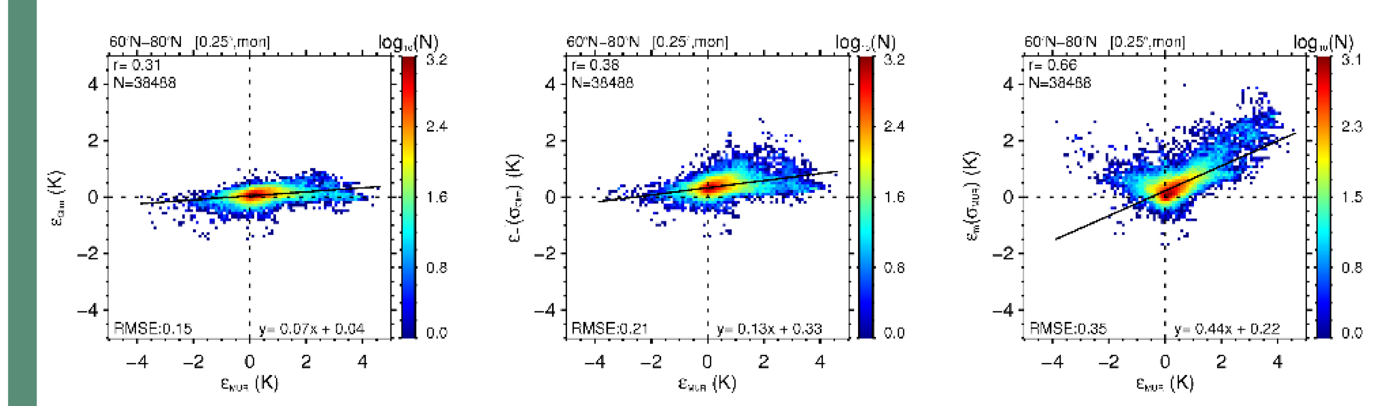

Figure 4. The 60ºN-80ºN summer month error estimates using ε_{clim} (first column), $\varepsilon_m{}'$ (second column), and ε_m (third column). r denotes the correlation coefficients; N is the total number of grids at the resolution [0.25º, mon]; RMSE and the fitting line are denoted at the bottom of each plot.

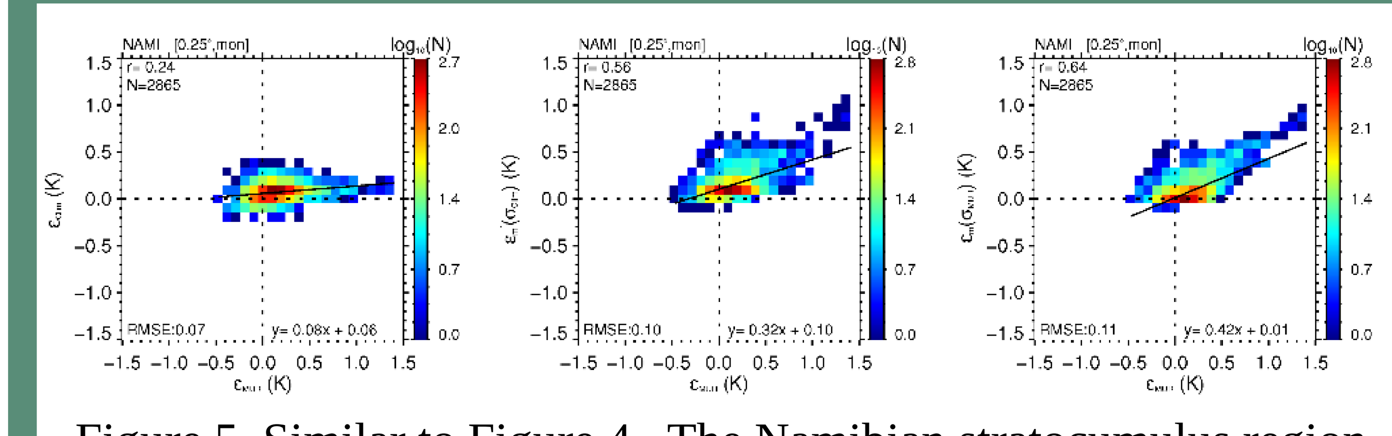

Figure 5. Similar to Figure 4 . The Namibian stratocumulus region sampling error estimates for October 2011 are shown.

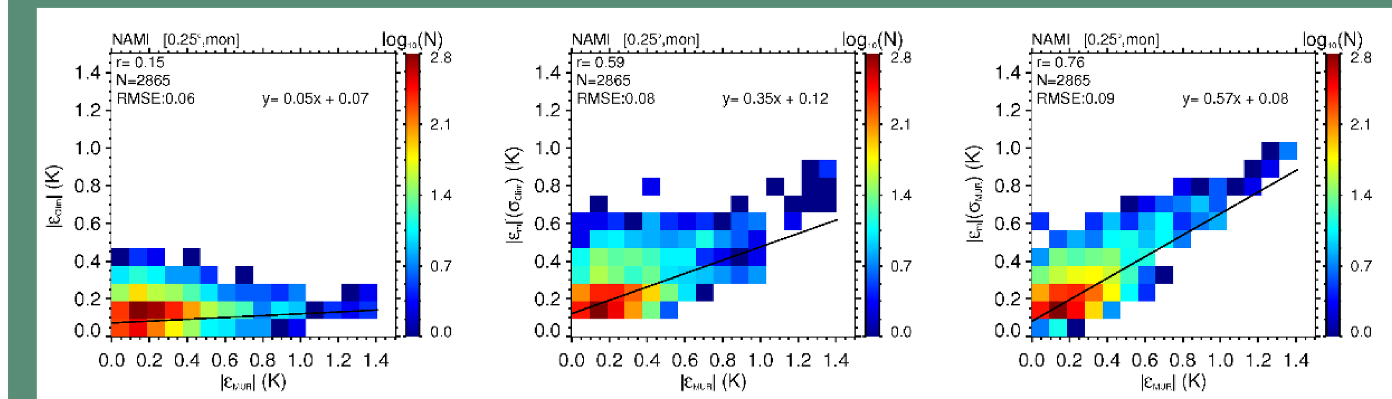

Figure 6. Similar to Figure 5 . The sampling error absolute values are estimated.

Discussion and Conclusions

We propose an empirical model that includes the climatology component as well as the sampling error dependence information from the MODIS cloud mask and the SST variability. For sampling errors due to temporal averaging, this model can largely improve the error estimation from by only using the climatology component of the sampling error, especially in regions where warm sampling errors are prevalent, but the training needs to be conducted using more data and more locally.

Reference

Banzon, V.F., Reynolds, R.W., Stokes, D., & Xue, Y. (2014). A 1/4°-Spatial-Resolution Daily Sea Surface Temperature Climatology Based on a Blended Satellite and in situ Analysis. Journal of Climate, 27, 8221-8228

Chin, T.M., Jorge, V., & Armstrong, E. (2010). Algorithm Theoretic Basis Document: Multi-scale, motion-compensated analysis of sea surface temperature Version 1.1.

Liu, Y., & Minnett, P.J. (2016). Sampling errors in satellite-derived infrared sea-surface temperatures. Part I: Global and regional MODIS fields. Remote Sensing of Environment, 177, 48-64